Table 2 Values of parameters in Eqs. (2) and (3), with $\sigma_0 \leqslant \sigma_L$

Structural metal	J_0	α	J_2	J_4	σ_L, psi
Grey iron	3.05×10^{-10}	2.45	94.4×10^{-10}	1.42×10^{-16}	6,500
Magnesium	15.6×10^{-10}	2.0	15.6×10^{-10}	0	8,000
1020 steel	5.22×10^{-10}	2.0	5.22×10^{-10}	0	30,000
Sandvick steel (Q-T)	1.5×10^{-10}	2.28	0.93×10^{-10}	1.57×10^{-20}	100,000

damping data to the biaxial stress case. One form of this statement which has been suggested is[4]

$$\sigma_n = (3\tau_m^2 + \lambda\, \sigma_d^2)^{1/2} \tag{9}$$

where

$\tau_m = (\sigma_1 - \sigma_2)/2$
$\sigma_d = (\sigma + \sigma_2)/2$
σ_1, σ_2 = principal stress amplitudes in biaxial stress state
λ = "curve-fitting" parameter for specific materials
σ_n = stress amplitude in uniaxial stress state, which produces the same energy dissipation

Recent tests[2] on thin-walled, cylindrical specimens of manganese alloy have shown a value of $\lambda = 1.2$.

Hypothesize the stress-strain relations to take the following form (only justification being resemblance to the elastic equations of plane stress and simplicity):

$$\begin{aligned} \sigma_x &= [E/(1-\nu^2)](\epsilon_x + \nu\epsilon_y) + E^*(\dot{\epsilon}_x + \nu^*\dot{\epsilon}_y) \\ \sigma_y &= [E/(1-\nu^2)](\epsilon_y + \nu\epsilon_x) + E^*(\dot{\epsilon}_y + \nu^*\dot{\epsilon}_x) \end{aligned} \tag{10}$$

where ν is Poisson's ratio and E^*, ν^* are two parameters introduced to allow some flexibility in incorporating the results of Eq. (3) through the use of Eq. (9). The approximation corresponding to $c^2\omega^2 \ll 1$ in the uniaxial case now takes the form $\omega(1+\nu)(1-\nu^*)\,E^*/E \ll 1$ and $\omega(1-\nu)(1+\nu^*)\,E^*/E \ll 1$, which leads to the following expressions for the arbitrary constants in Eq. (10):

$$E^* = \frac{E}{\pi\omega}\left[\frac{\lambda}{(1-\nu)^2} + \frac{3}{(1+\nu)^2}\right][J_2 + E\,J_4\,(\epsilon_{0x}^2 + 2\,\nu^*\epsilon_{0x}\epsilon_{0y} + \epsilon_{0y}^2)]$$

$$\lambda^* = \frac{\lambda\,(1+\nu)^2 - 3\,(1-\nu)^2}{\lambda\,(1+\nu)^2 + 3\,(1-\nu)^2}$$

where ϵ_{0x} and ϵ_{0y} are the amplitudes of the principal strains.

Concluding Remarks

Although the foregoing developments are essentially heuristic, combining both curve fitting of experimental results and arbitrary construction of constitutive equations, they enable immediate application of published damping data to be made in vibration analysis. The complexity of the equations, admittedly, precludes any elementary development of vibration response curves. Certain limited results, such as the steady-state response in the neighborhood of a resonance, however, are obtained quite easily, particularly for single structures such as a beam or plate. The technique is to use asymptotic expansions to generate successively higher order approximations of the solution.

Analysis of vibrations response problems using the stress-strain relations developed in this note have been carried out for the uniaxial stress case in Ref. 5 and for a biaxial stress case in Ref. 6. In particular, these solutions were for the steady-state response of a cantilever beam that was excited in bending by a rotational oscillation of its base and for the steady-state response of a circular plate that was excited by pulsating pressure loading. One observation stemming from this latter work was that the parameters to be used in the asymptotic expansions must be chosen carefully in order to avoid the higher ordered approximations from being singular.

References

[1] Lazan, B. J., "Damping and resonant fatigue in metals," *Proceedings of the International Congress on Fatigue of Metals* (The Institution of Mechanical Engineers, London, September 1956), pp. 90–101.

[2] Mentel, T. J. and Chi, S. H., "Experimental study of dilatational versus distortional straining action in material damping production," Paper V8, 65th Meeting of the Acoustical Society of America, New York (May 1963).

[3] Whittier, J. S., "Hysteretic damping of structural materials under biaxial dynamic stress," Exptl. Mech. **2**, 321–328 (November 1962).

[4] Mentel, T. J., "Vibrational energy dissipation at structural support junctions," *Structural Damping*, edited by J. E. Ruzicka (American Society of Mechanical Engineers, New York, 1959), pp. 89–116.

[5] Mentel, T. J. and Fu, C. C., "Analytical formulation of damped stress-strain relations based on experimental data with applications to vibrating structures," Aeronautical Systems Div. TR 61-623 (November 1961).

[6] Fu, C. C., "Response of circular plates exhibiting generalized boundary damping and empirically based material damping," Aeronautical Systems Div. TR 61-647 (November 1961).

Free-Molecule Flow through Inlet Scoops

Y. C. WHANG*
Catholic University of America, Washington, D. C.

THIS note is concerned with flow through inlet scoops under free-molecule condition. An inlet scoop is a converging conical duct with the larger end open to the freestream and the smaller end connected to a chamber. The freestream flow is maintained at velocity U, pressure p_∞, and temperature T_∞. The macroscopic velocity U is supposed to be parallel to the longitudinal axis of the scoop. While in the chamber, the pressure and temperature are maintained at p_c and T_c. A steady state has been attained.

At first glance, it might be supposed that with a proper design of the geometry the net rate of mass flow through a scoop will depend mainly on the cross-sectional area of the scoop opening A_1, and, hence, substantial increases in the net rate of mass flow passing through the throat inlet with the aid of big scoops are expected. Rather surprisingly, this analysis indicates that in the free-molecule flow regime the gain of mass flow due to "scoop action" never can exceed a factor of two. Therefore, increases of mass flow into the chamber can be achieved by increasing the size of the throat inlet area A_2 rather than by using a big scoop. However, if the throat inlet area is fixed, for any scoop length an optimum scoop geometry can be found through which a relatively maximum mass flow rate can be attained.

Received by IAS October 23, 1962; revision received May 17, 1963. This study was conducted at the National Engineering Science Company, Pasadena, Calif., during the summer of 1962.

* Assistant Professor, Division of Space Science and Applied Physics. Member AIAA.

It is assumed that the molecules in the chamber will achieve Maxwellian equilibrium conditions before passing into the scoop, and that molecules are reflected diffusely from the wall with a Maxwellian velocity distribution. In the control volume bounded by A_1, A_2, and the inner wall of the scoop A_w, the mass of molecules leaving A_w and A_2 is proportional to the cosine of the angle with respect to the normal to the surface. This appears quite similar to the process of heat radiation in the same control volume from the black surfaces A_w and A_2. The rate at which the mass of molecules enters the scoop from the chamber may be assumed to be distributed uniformly across A_2. However, the mass of molecules leaving a unit area of the wall surface per unit time is more likely a decreasing function along the longitudinal axis of the scoop. In the analysis to be carried out here, the leaving mass flux from A_w is approximated by its mean value over the whole inner wall. The error introduced by this approximation is small when the scoop length is not larger than the diameter of the scoop inlet area. Because of the uniform distribution of leaving mass flux over A_w and A_2, respectively, the similar process of heat radiation in the same control volume from the black surfaces A_w and A_2 is simplified to the case in which the two black surfaces A_w and A_2 are kept at different but constant temperatures.

The similarities between the transport processes in free-molecule flow regime and by thermal radiation[1, 2] are used in carrying out this analysis. Let L denote the length of the scoop and r_1 and r_2 denote the radii of A_1 and A_2, respectively; then a formula [Eq. (9)] is obtained to express the net rate of mass flow through inlet scoop as a function of the scoop geometry (L, r_1, r_2), the freestream conditions (U, p_∞, T_∞), and the chamber conditions (p_c, T_c); thus the optimum geometries are established for various freestream conditions.

In this paper, a Cartesian coordinate system with respect to scoop with the z axis parallel to the axis of the scoop is used. Since there are no intermolecular collisions across the scoop opening section A_1, the distribution function f_1 in the half space $V_z > 0$ must not be distorted due to the presence of the scoop and the chamber. Therefore, $f_1 = f_\infty$ for $V_z > 0$, where f_∞ is the distribution function for the molecular velocities in the freestream. Let $M_{\infty-1}$ denote the rate at which the mass of molecules pass through A_1 directly from the freestream, M_{c-1} denote the rate at which the mass of molecules leaving the chamber will pass directly through A_1, and M_{w-1} denote the rate at which the mass of molecules reflected from the wall will pass directly through A_1. Then, the net rate of mass flow across A_1 can be written as

$$M = M_{\infty-1} - M_{c-1} - M_{w-1} \tag{1}$$

in a steady state; this represents the net rate of mass flow through the inlet scoop. $M_{\infty-1}$ can be carried out as

$$M_{\infty-1} = [\pi r_1^2 p_\infty/(2\pi RT_\infty)^{1/2}][e^{-S^2} + (\pi)^{1/2}S(1 + \text{erf}S)] \tag{2}$$

Here the quantity S denotes the "speed ratio," which is the ratio of the freestream velocity U to the most probable random speed in the freestream $(2RT_\infty)^{1/2}$. The freestream molecules entering section A_1 will either fall directly on section A_2 without hitting the scoop wall or fall directly on the wall. Let $M_{\infty-2}$ denote the rate at which the mass of molecules from the freestream directly enters the chamber through A_2 without hitting the wall. Since for the scoops, which are of interest here, A_2 is always smaller than A_1, the rate at which the freestream molecules directly enter the chamber through A_2 is considered to be distributed uniformly over A_2 and to be equal to its corresponding value at the center of A_2. One can obtain

$$M_{\infty-2} = \frac{\pi r_2^2 p_\infty}{(2\pi RT_\infty)^{1/2}}\left[\frac{r_1^2 e^{-S^2}}{L^2 + r_1^2} + (\pi)^{1/2}S\left\{1 + \text{erf}S - \left(\frac{L}{(L^2 + r_1^2)^{1/2}}\right)^3\left(1 + \text{erf}\frac{LS}{(L^2 + r_1^2)^{1/2}}\right)e^{-r_1^2S^2/(L^2+r_1^2)}\right\}\right] \tag{3}$$

The gas in the chamber is considered to be in Maxwellian equilibrium. Let M_{c-2} denote the rate at which the mass of molecules leave the chamber through A_2, M_{c-1} denote the rate at which the mass of molecules from the chamber leave A_1 directly without hitting on the wall, and $\bar{F}_{2-1}$ denote the mean shape factor of area A_2 against A_1 in thermal radiation. It has been established that

$$M_{c-2} = \pi r_2^2 p_c/(2\pi RT_c)^{1/2} \tag{4}$$

and[3]

$$\bar{F}_{2-1} = (L^2 + r_1^2 + r_2^2 - \phi^2)/2r_2^2 \tag{5}$$

where

$$\phi^2 = [(L^2 + r_1^2 + r_2^2)^2 - 4r_1^2r_2^2]^{1/2}$$

Since the transport of molecules from A_2 shares similarities with energy transport by thermal radiation, M_{c-1} can be obtained immediately as the product of M_{c-2} and $\bar{F}_{2-1}$, that is,

$$M_{c-1} = [\pi p_c/(8\pi RT_c)^{1/2}](L^2 + r_1^2 + r_2^2 - \phi^2) \tag{6}$$

From the requirement of mass conservation, the sum of $(M_{\infty-1} - M_{\infty-2})$ and $(M_{c-2} - M_{c-1})$, which represents the mass of molecules incident on the scoop wall directly from the freestream and the chamber in a unit time, must equal the rate at which the mass of molecules reflected from the wall directly falls on A_1, M_{w-1}, plus that at which it directly falls on A_2, M_{w-2}. Now, if a scoop geometry factor is introduced,

$$\sigma = M_{w-2}/(M_{w-1} + M_{w-2})$$

then the net rate of mass flow through the scoop [Eq. (1)] can be expressed as

$$M = (1 - \sigma)(M_\infty - M_{c-1}) + \sigma(M_{\infty-2} - M_{c-2}) \tag{7}$$

The scoop geometry factor σ can be evaluated by making use of the similarities with thermal radiation; the expression for σ is

$$\sigma = (\phi^2 - L^2 + r_1^2 - r_2^2)/[2(\phi^2 - L^2)] \tag{8}$$

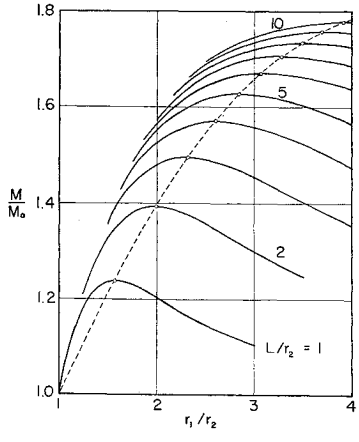

Fig. 1 Mass flow rate vs r_1/r_2 for $S = 5$ and $p_c = 0$.

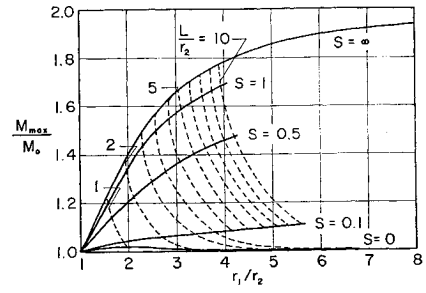

Fig. 2 Design data for optimum inlet scoops.

Substitution of Eqs. (2–4, 6, and 8) into (7) yields the expression for the net rate of mass flow through inlet scoop:

$$M = \frac{\pi r_2^2 p_\infty}{(2\pi RT_\infty)^{1/2}} \left\{ C_1 e^{-S^2} + C_2(\pi)^{1/2} S(1 + \text{erf}S) - C_3(\pi)^{1/2} S \left[1 + \text{erf} \frac{LS}{(L^2 + r_1^2)^{1/2}} \right] e^{-r_1^2 S^2/(L^2 + r_1^2)} - C_4 \frac{p_c}{p_\infty} \left(\frac{T_\infty}{T_c} \right)^{1/2} \right\} \quad (9)$$

where

$$C_1 = \frac{r_1^2[(L^2 + r_1^2 + r_2^2)\phi^2 - (L^2 + r_1^2)^2 + 2r_1^2 r_2^2 - r_2^4]}{2r_2^2(L^2 + r_1^2)(\phi^2 - L^2)}$$

$$C_2 = \frac{r_1^2 + r_2^2}{2r_2^2} - \frac{(r_1^2 - r_2^2)^2}{2r_2^2(\phi^2 - L^2)}$$

$$C_3 = \frac{L^3(\phi^2 - L^2 + r_1^2 - r_2^2)}{2(\phi^2 - L^2)(L^2 + r_1^2)^{3/2}}$$

$$C_4 = \frac{(L^2 + r_1^2 + r_2^2)\phi^2 - \phi^4}{2r_2^2(\phi^2 - L^2)}$$

If no inlet scoop is used, Eq. (9) reduces to the expression for the mass flow rate through a circular aperture of negligible lip thickness:

$$M_0 = [\pi r_2^2 p_\infty/(2\pi RT_\infty)^{1/2}] \; [e^{-S^2} + (\pi)^{1/2} S(1 + \text{erf}S)] \quad (10)$$

The dimensionless mass flow rate through inlet scoop is defined as the ratio of M to M_0. For any given value of S and $(p_c/p_\infty)/(T_\infty/T_c)^{1/2}$, the mass flow rates can be plotted as functions of scoop geometry (i.e., L/r_2 and r_1/r_2, e.g., see Fig. 1). From these curves it can be seen that, for any given scoop length ratio (L/r_2), there exists an optimum scoop geometry through which the mass flow rate reaches a maximum value.

It is coincident with the author's intuitive prediction that the maximum mass flow rate increases as the size of the scoop and the freestream velocity ratio increase. However, when S approaches infinity and $r_1^2 = r_2^2 + (2r_2^2 + 2L^2)^{1/2}$, then M/M_0 attains a maximum value

$$\lim_{S \to \infty} \left(\frac{M_{\max}}{M_0} \right) = \frac{2L^2 + 3r_2^2 + 2(2r_2^2 + 2L^2)^{1/2}}{L^2 + 2r_2^2 + 2(2r_2^2 + 2L^2)^{1/2}}$$

From this one can see clearly that the gain of mass flow rate with the aid of a big scoop is limited by a factor of two.

In the design of inlet scoops, for any given value of L/r_2 a family of curves for M/M_0 vs r_1/r_2 may be plotted. For $S > 1$, the maximum mass flow rates occur almost at the same value of r_1/r_2, and, for $S > 2$, all curves are very close to one another. As an example, when $L/r_2 = 2$, the maximum mass flow rate can be maintained for a very wide range of freestream velocity when $r_1/r_2 = 1.98$, and, for $S > 2$, the mass flow rate through this inlet scoop can be represented by a simple formula:

$$M = 1.392 \; \rho_\infty U_\infty A_2$$

Numerical solutions for the dimensionless mass flow rate through optimum inlet scoops are obtained and plotted in Fig. 2, which is useful for the design of optimum inlet scoops at various lengths.

A similar problem concerning the free-molecule flow through a diverging duct for $S = 0$ was treated by Davis et al.,[4] who obtained some exact numerical solutions by using the Monte Carlo method. In this note the problem is treated analytically based on two important assumptions: 1) the mass flux incident on the wall is uniform, and 2) the mass flux passing directly from A_1 to A_2 without striking the wall is equal to the mass flux passing the midpoint of A_2. When $S = \infty$, these two assumptions represent the true case, and the result obtained here gives the exact solution of the problem. However, when $S = 0$, the result obtained here does not agree very well with Davis' solution, because of the two forementioned assumptions. It is believed that, if S is not very small, say $S > 1$, the result obtained here will be quite accurate for optimum geometries.

References

[1] Eckert, E. R. G., "Similarities between energy transport in rarefied gases and by thermal radiation," *Modern Developments in Heat Transfer* (Academic Press, New York, 1962), pp. 159–180.

[2] Sparrow, E. M., Jonsson, V. K., and Lundgren, T. S., "Free-molecule tube flow and adiabatic wall temperatures," AMSE-AIChE Heat Transfer Conference, Houston, Texas (August 5–8, 1962), Paper 62-HT-35.

[3] Eckert, E. R. G. and Drake, R. M., *Heat and Mass Transfer* (McGraw-Hill Book Co. Inc., New York, 1959), p. 398.

[4] Davis, D. H., Levenson, L. L., and Milleron, N., "Theoretical and experimental studies of molecular flow through short ducts," *Rarefied Gas Dynamics*, edited by L. Talbot (Academic Press, New York, 1961), pp. 99–115.

Impact Force and Crater Surface Area

R. F. Rolsten* and H. H. Hunt†

General Dynamics/Astronautics, San Diego, Calif.

Nylon, glass, and aluminum projectiles impacting on aluminum at velocities of 3.78 to 5.43 × 10^5 cm/sec produce hemispherical craters. The impact damage can be related to the tensile strength by using equations for uniformly accelerated rectilinear motion when the measured crater dimensions are corrected for relaxation after the pressure release. Steel projectiles do not conform to this impact model.

Nomenclature

P = pressure applied to the target, dynes/cm^2
A = surface area of crater, cm^2
F = force applied to the target, dynes
W = work
m = mass of projectile, g
v = velocity of projectile, cm/sec
d = distance (penetration depth or radius of the hemispherical crater) through which the force is applied, cm
d' = projectile diameter, cm
a = acceleration (or deceleration), cm/sec^2
ρ_P = projectile density, g/cm^3
ρ_T = target density, g/cm^3
C_T = speed of sound in target, cm/sec

Introduction

BEHAVIOR of materials subjected to high velocity impact (impulsive loading) has led to concepts that do not follow conventional loading problems. These concepts depend upon the elements of time and motion. Thus, when a material is subjected to an impulsive load (element of time), the motion may attain a value that is critical with regard to the initiation of a specific mode of behavior.

The effect of high pressure on the bulk physical and mechanical properties may be very pronounced under impulsive loading since pressures of several hundred thousand pounds per square inch are attained frequently. Peak pressures are attained in about 10^{-6} to 10^{-7} sec. These high pressure

Received by IAS November 20, 1962; revision received June 4, 1963.

* Associate Professor at California Western University.

† Chemist.